A Practical Guide for Predicting the Stereochemistry of Bifunctional Phosphoric Acid Catalyzed Reactions of Imines

Jolene P. Reid,[†] Luis Simón[‡] and Jonathan M. Goodman[†]*

[†]Centre for Molecular Informatics, Department of Chemistry, University of Cambridge, Lensfield Road, Cambridge CB2 1EW, United Kingdom

[‡]Facultad de Ciencias Químicas, Universidad de Salamanca, Plaza de los Caídos 1-5, Salamanca E37004, Spain

jmg11@cam.ac.uk

CONSPECTUS

Chiral phosphoric acids have become powerful catalysts for the stereocontrolled synthesis of a diverse array of organic compounds. Since the initial report, the development of phosphoric acids as catalysts has been rapid, demonstrating the tremendous generality of this catalyst system and advancing the use of phosphoric acids to catalyse a broad range of asymmetric transformations ranging from Mannich reactions to hydrogenations through complementary modes of activation. These powerful applications have been developed without a clear mechanistic understanding of the reasons for the high level of stereocontrol.

This account describes investigations into the mechanism of the phosphoric acid catalyzed addition of nucleophiles to imines, focussing on binaphthol-based systems. In many cases, the hydroxyl phosphoric acid can form a hydrogen bond to the imine whilst the P=O interacts with the nucleophile. The single catalyst, therefore, activates both the electrophile and the nucleophile, whilst holding both in the chiral pocket created by the binaphthol and constrained by substituents at the 3 and 3' positions.

Detailed geometric and energetic information about the transition states can be gained from calculations using ONIOM methods that combine the advantages of DFT with some of the speed of force fields. These high-level calculations give a quantitative account of the selectivity in many cases, but require substantial computational resources. A simple qualitative model is a useful complement to this complex quantitative model.

We summarize our calculations into a working model that can readily be sketched by hand and used to work out the likely sense of selectivity for each reaction. The steric demands of the different parts of the reactants determine how they fit into the chiral cavity and which of the competing pathways is favored. The preferred pathway can be found by considering the size of the substituents on the nitrogen and carbon atoms of the imine electrophile, and the position of the nucleophilic site on the nucleophile in relation to the hydrogen-bond which holds it in the catalyst active site.

We present a guide to defining the pathway in operation allowing the fast and easy prediction of the stereochemical outcome and provide an overview of the breadth of reactions that can be explained by these models including the latest examples.

INTRODUCTION

Chiral phosphoric acids (CPA) have become very popular catalysts in organic synthesis. The addition of nucleophiles to imines is an important field and constitutes the largest substrate class for these reagents. A variety of nucleophiles have shown to participate efficiently, enabling the formation of multiple types of bonds, (C-C, C-O, C-S, C-N, C-P and C-H) in an asymmetric fashion (**Figure 1**). The versatility, mild conditions and functional group tolerance makes this type of catalyst very appealing. The stereochemical outcome in these reactions is controlled by the substituents at the 3,3' position. Although no catalyst is optimal for all combination of reactants, large

substituents are required for high stereoselectivity. TRIP, which was developed by List[1] and has 2,4,6-triisopropylphenyl groups in the 3 and 3' positions, is by far the most versatile and selective catalyst reported to date.
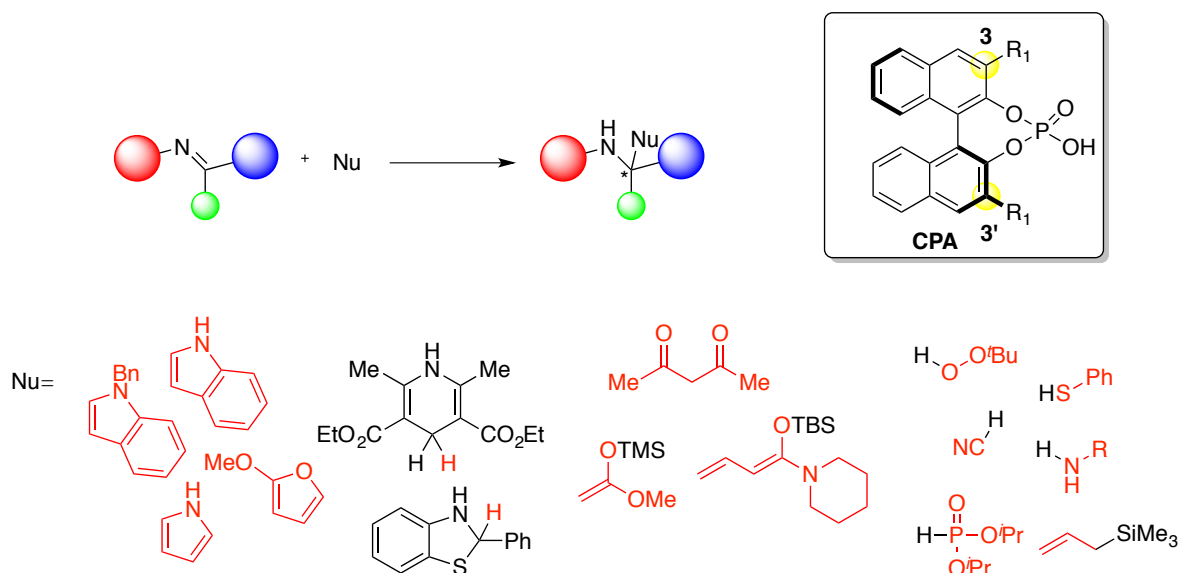

Figure 1. Examples of nucleophilic addition imines catalyzed by phosphoric acids. Red indicates the functionality added to imine.

Phosphoric acids catalyse these transformations through multiple mechanisms and numerous experimental and computational studies are now generating a good mechanistic understanding of the reasons for stereoselectivity. Several review articles summarize the wide variety of reactions;[2-3] recent reviews have focused attention on defining reactions by mode of activation.[4-5] This is an account of computational investigations using QM/MM hybrid methods into understanding the mechanism and origins of enantioselectivity. The results of the calculations are summarized into a simple qualitative model allowing the rapid prediction of stereoselectivities.

PHOSPHORIC ACID CATALYZED TRANSFER HYDROGENATION

The transfer hydrogenation of imines by Hantzsch esters was an early example of a transformation catalyzed by phosphoric acids (**Figure 2**).[6-8] At that time there were two plausible mechanisms (**Figure 3**). The first, *Mechanism_A*, involves activation of the imine through a single hydrogen bond, in which the Hantzsch ester approach should be preferred on one face. An alternative, *Mechanism_B*, involves the activation of both the electrophile and the nucleophile by the catalyst. Investigations on the Mannich,[9] aza-ene,[10] Friedel-Crafts,[11] and hydrophosphonylation[12] reactions have also concluded a similar mechanism could be in operation. We expressed a preference for *Mechanism_B*, as the substrate bound to the catalyst *via* a single hydrogen bond was too flexible to account for the high enantioselectivity, although there was experimental evidence based on X-ray diffraction studies of imine-catalyst complex in support of *Mechanism_A*.[8] Terada *et al*. also suggested that a similar process to *Mechanism_A* could be in operation in the Mannich reaction.[13-14] Yamanaka and Akiyama have proposed activation by bifunctional coordination to an imine.[15] We label this *Mechanism_A* rather than *Mechanism_B* because only the electrophile is activated not both the electrophile and the nucleophile.
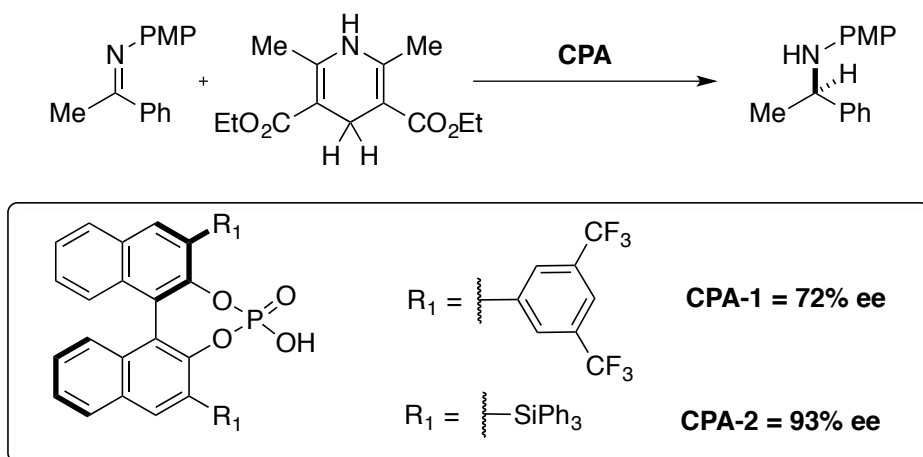
Figure 2. BINOL-phosphoric acid catalyzed transfer hydrogenation. The MacMillan synthetic protocol[8] differs from the Rueping approach[6] as the imines were not pre-formed. The overall transformation, however, was the same.

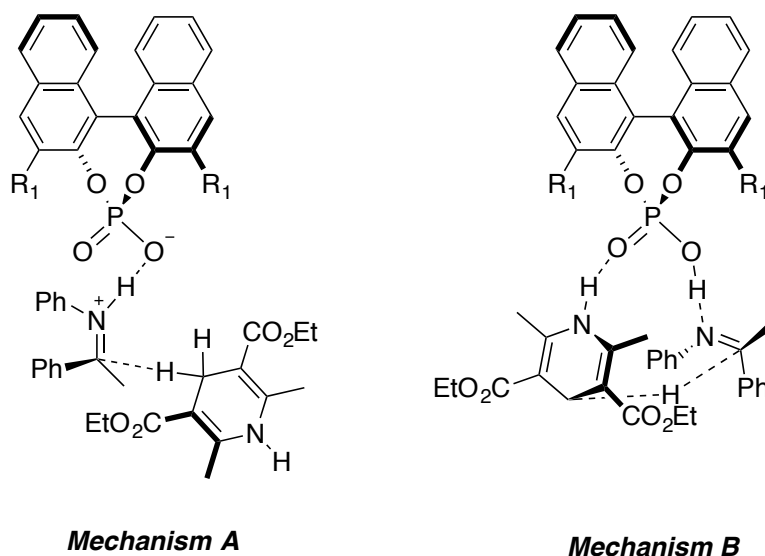
Mechanism A

Mechanism B

Figure 3. Mechanistic proposals for the transfer hydrogenation reaction

Using a simplified model, 1,3-butadiene-1,4-diol-phosphoric acid, as the catalyst we calculated which of the mechanisms was most likely using DFT (**Figure 4**).[16] The study revealed four unique transition states for *Mechanism_B*, evenly divided between *E* and *Z* configurations of the imine. Due to the open, flexible, nature of *Mechanism_A*, twelve transition states were found, also evenly divided between *E* and *Z* imine configurations. The relative energies of these competing transition states showed that *Mechanism_A* was strongly disfavored relative to *Mechanism_B*, where the hydrogen atoms are transferred between reactants and catalyst in a concerted fashion. Another possible mode of activation involves protonation of imine and a single interaction from the phosphate catalyst with NH of the Hantzsch ester; we call

this *Mechanism_C*. As with *Mechanism_A*, *Mechanism_C* was strongly disfavored relative to *Mechanism_B*. The transition structures in which the imine has a *Z* configuration are lower in energy compared to *E*. Although calculations show that the *E*–imine ground state is more stable by 2.9 kcal mol^{-1}, a fast *E/Z* equilibration is expected and so the reaction should proceed through the lowest transition state pathway, following the Curtin-Hammett principle. Mechanisms have been reported for the acid catalyzed *E/Z* isomerisation of imines, including protonation-rotation and addition-rotation-elimination.[17] Lack of resonance stabilization and greater steric interactions between the phenyl and methyl groups in the imine all contribute to the destabilisation of the *E* transition state. Rueping constructed a model based on an X-ray crystal structure of the phosphoric acid catalyst.[6] In this model, he placed the imine in a *Z* configuration and the nucleophile approached from the less-hindered face, reproducing the sense of stereoinduction observed experimentally.
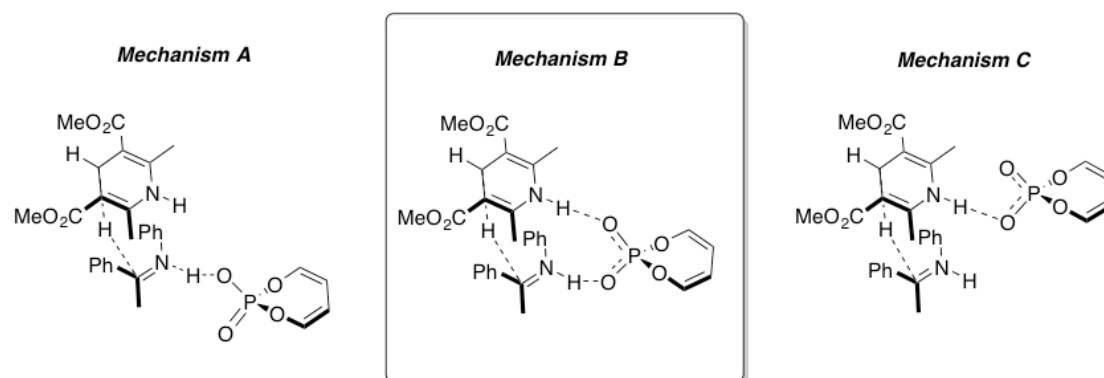

Figure 4. Lowest energy transition states for the model catalyst

Model for Stereoselectivity

To probe the origins of stereoselectivity transition states using the full catalyst system were located. To reduce computational time, simpler molecules were used as

substrates in the calculations: para-methoxyphenyl (PMP) was replaced by phenyl; dimethyl Hantzsch ester was used instead of diethyl. We performed high-level two-layer ONIOM calculations using the Gaussian package.[18] Our group has successfully investigated the enantiodetermining step of many phosphoric acid catalyzed reactions using this method.[16,19-24] These calculations demonstrated that molecular mechanics, despite being computationally very cheap, was sufficiently accurate to describe the steric environment of the BINOL scaffold; the chemically relevant part, bond breaking and making, was investigated using QM methods (Figure 5). A benchmarking process determined UFF offered a better description of the rotational barrier of biphenyl when compared to semiempirical methods, so it reproduces well the position of the bulky groups attached to the BINOL. The failures of popular density functionals, including B3LYP,[25-26] to describe dispersion effectively are well documented[27] and this has the result that the prediction of critical binding energies is too small in many reactions. The Minnesota meta-GGA functionals developed by Truhlar,[28-29] have been parameterized to include dispersion effects and their use has become routine in the study of dispersion dominated systems. Geometry optimization with ONIOM(B3LYP/6-31G(d):UFF) followed by single-point calculations (MPWB1K/6-31G**) in toluene with polarizable continuum model (PCM) was performed in this study. By combining MM and QM, the speed of the calculations is dramatically increased without compromising the precision for this many-atom system. The additional single-point calculation is required to accurately describe the multiple interactions leading to overall catalytic effect. Applying this energy correction allows improved comparisons of calculation with experiment.
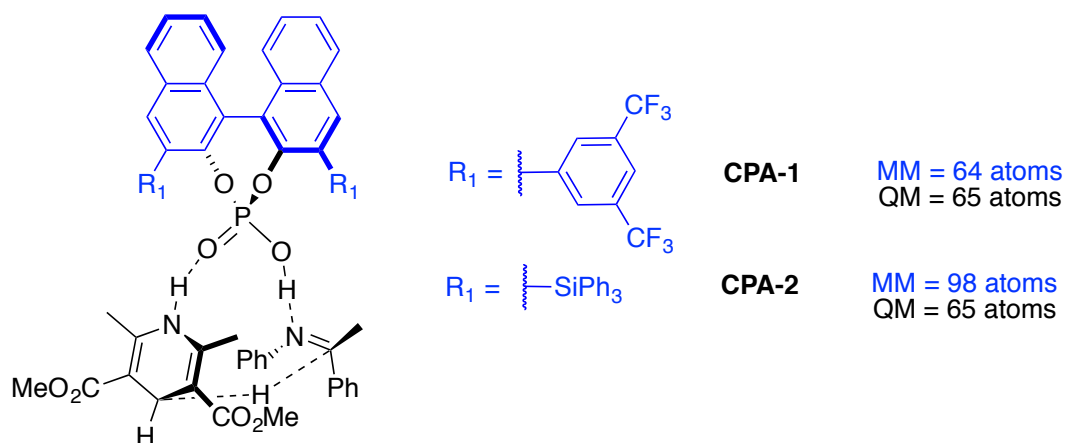
Figure 5. ONIOM partitioning in the phosphoric acid catalyzed transfer hydrogenation. Blue indicates atoms treated with MM; black indicates atoms treated with QM.

Computations of the full catalyst systems have led to the development of the model depicted in **Figure 6**. This is based on a projection of the catalyst such that both the BINOL oxygens are in the plane of the paper. The free oxygens are above and below, each having bulky substituents on either side. Alternatively, the chiral scaffold can be modelled by a quadrant diagram, in which quadrants I and IV are equivalently hindered. The reagents reside in the empty quadrants. Such a model originally proposed by Terada[14] and Himo [30] has become popular to explain the stereoselectivities of numerous phosphoric acid catalyzed reactions.

Goodman Projection - looking across the C_2 symmetric axis
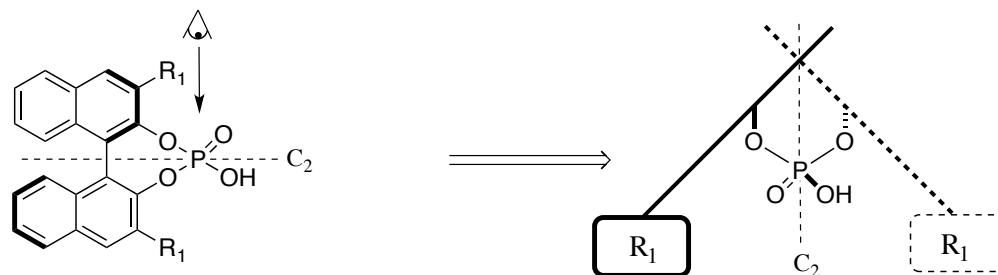
Quadrant Projection - looking down the C_2 symmetric axis

I
Filled Quadrant

II
Empty Quadrant

III
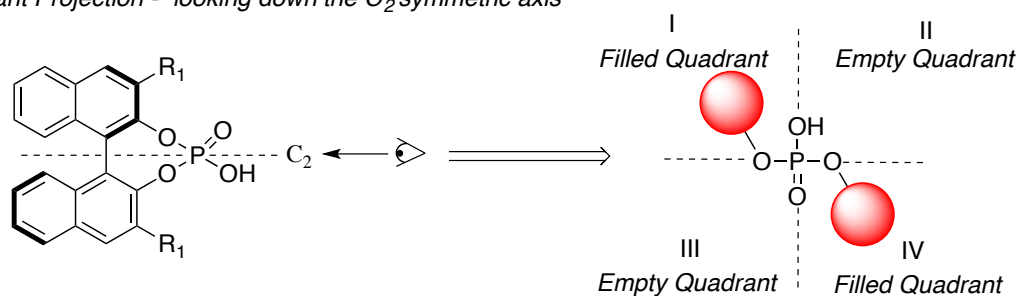*Empty Quadrant*

IV
Filled Quadrant

Figure 6. Alternative views of the phosphoric acid catalyst

The catalyst binds to the substrate *via* the catalyst hydroxyl group and there is a second interaction from the phosphoryl oxygen to the nucleophile proton. The C_2 symmetry of the phosphate anion allows us to draw the imine at the front of the diagram without loss in generality. The *N*-substituent can be directed away from the front of the 3,3' which we label *Type I* or towards the 3,3' which we label *Type II*. Additionally, the imine can exist as the *E* or *Z* stereoisomers, which is defined based on steric size. In each case the nucleophile is delivered from behind (Figure 7).

Figure 7. Transition state models for the prediction of stereoselectivity

Both catalysts favored a *Type I Z* pathway. Several interactions account for such a preference. The unfavorable steric clash between the large phenyl substituent and the 3,3' disfavors the *E* transition state relative to the *Z*. Similar steric interactions between the *N*-substituent and the 3,3' group disfavors *Type II* relative to *Type I*.

The calculations also capture the increase in stereoselectivity observed when MacMillan's catalyst (**CPA-2**: Figure 2, $R_1 = SiPh_3$) was employed. Relative populations of transition states were predicted at the temperature they were performed from electronic energy differences and based on Boltzmann distribution analysis. The

computed enantiomeric excess (ee) for Rueping's catalyst (**CPA-1**: Figure 2, R_1 is phenyl with two meta-CF_3 groups) was 70 % ee and 97 % ee for MacMillan's (**CPA-2**), which are very close to the experimental values, 72 % and 93 %, respectively (**Figure 2**). List and co-workers reported a similar protocol to Rueping's.[7] Improved enantioselectivities were reported when TRIP (**CPA-4**: Figure 1, R_1 is tri-isopropyl-phenyl) was used as the catalyst. Although the precise mechanism was unclear, the Rueping group expanded the scope of the transfer hydrogenation to quinolines.[31] In such a substrate only the *Z* imine configuration could exist. This produced the same sense of stereoinduction as with the transfer hydrogenation reaction, which provides further evidence of the participation of a *Z* imine in the transition state, reinforcing Rueping's original suggestion. Himo *et al*. also observed through DFT calculations that the chiral phosphate acts as a bifunctional catalyst in their theoretical study of the transfer hydrogenation reaction of phenyl ketimines.[30] Expressing the importance of *E* and *Z* imine stereoisomers for the stereochemical induction, the group determined that the more compact *Z* iminium transition state was energetically more feasible than *E*. Yamanaka *et al*. have reached similar conclusions in their theoretical investigation into the mechanism of transfer hydrogenation of ketimines by benzothiazoline.[32] In their studies they also investigated the substituent effect of the phosphoric acid. Through calculating the diastereomeric transition state structures for each of the catalysts it was determined that the larger substituent enforces stereoselectivity. The 4.9 kcal mol^{-1} energy difference between the *Type I Z* and *Type II Z* in the TRIP catalyzed process is reduced to 1.5 kcal mol^{-1} with the 9-anthryl derived catalyst reproducing the trend observed experimentally. Shortly after the emergence of chiral phosphoric acid catalyzed transfer hydrogenations, the List group expanded this further with their investigations of the asymmetric reductive amination of aldehydes

via dynamic kinetic resolution. [33] A crucial practical requirement was the hydrogenation would be faster for one imine enantiomer than the other. Under reductive amination conditions rapid racemisation of the imine would occur through imine/enamine tautomerisation, setting up a dynamic kinetic resolution. Using this system, good to excellent enantioselectivities were achieved with a range of substrates. Detailed calculations by Himo have investigated the origins of enantioselectivity, in which they determine that the reaction proceeds through the *S-E*-imine.[34]

PHOSPHORIC ACID CATALYZED STRECKER REACTION

Our discoveries about the Hantszch ester hydrogenation lead us to re-examine the related Strecker reactions reported by Rueping (**Figure 8**).[35-36] Both imines undergo stereoselective cyanide addition to afford the corresponding α-aminonitriles in good to excellent enantiomeric excess. The reaction of ketimines lead to lower levels of selectivity and modification of the 3,3' substituent did not lead to an improvement. Intriguingly, the reaction of imine **1** produces the opposite sense of stereoinduction than the transfer hydrogenation reactions (**Figure 2**).[35] Recognizing this, the authors constructed a model based on the X-ray crystal structure of the phosphoric acid, in which the imine was in the *E* configuration and the nucleophile approached from the less hindered face. The configuration of the stereogenic center in **4** was not determined.
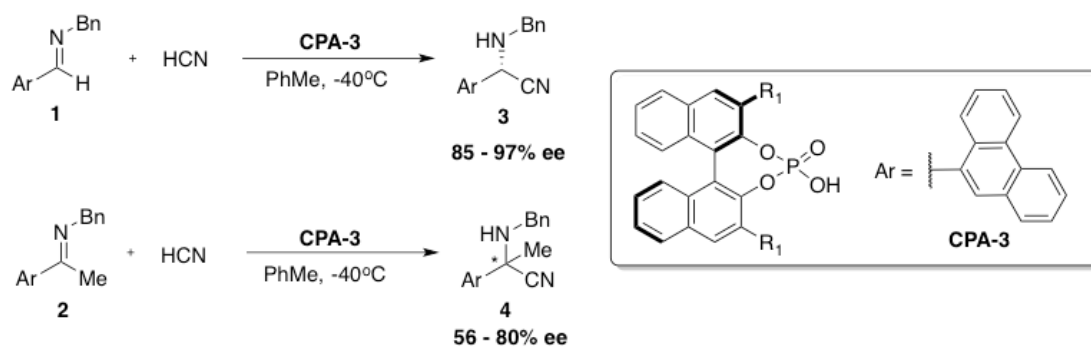
Figure 8. Examples of phosphoric acid catalyzed Strecker reactions reported by Rueping.[35-36]

Rueping proposed a stepwise mechanism, in which the phosphoric acid catalyst initally protonates the imine, activating it towards nucleophilic attack by the hydrogen cyanide. Recovering the proton from the protonated nucleophile then regenerates the phosphoric acid. The mechanism could also proceed through simultaneous hydrogen bonding interactions to electrophile and nucleophile analogous to our studies with the transfer hydrogenation of imines.[16] The preferred reaction pathway was determined using the model phosphoric acid as before. We considered four pathways summarized in **Figure 9.** Transition states in which the catalyst establishes a single interaction with HCN lead to *Mechanism_D*. The catalyst can establish two points of contact to the reactants leading to *Mechanism_E*. This would afford an alkylisocyanide that could rearrange to form the product.[37] These transition states were calculated to be disfavored relative to *Mechanism_F* in which the catalyst binds to hydrogen isocyanide through the phosphoryl oxygen and a second interaction from the Brønsted acidic site to the imine. This analysis suggests that the isomerisation of hydrogen cyanide is faster than the addition to the imine. The calculated energy barrier for

isomerization catalyzed by the phosphoric acid is 23.5 kcal mol^{-1}. Amines generated in the reaction may also participate in this process. The energy barrier mediated by ammonia was calculated to be 19.9 kcal mol^{-1}. The energy barrier for isomerisation is smaller than any of the reactions involving hydrogen cyanide suggesting a rapid isomerisation followed by addition. HCN attacking through the carbon rather than the nitrogen leads to *Mechanism_G*. The *Z* transition state corresponding to *Mechanism_G* was never located; attempted geometry optimisation led to rearrangement to the isomeric *Mechanism_F Z* TS. As with the transfer hydrogenation of phenyl ketimines, the model studies showed a preference for a *Z* TS.
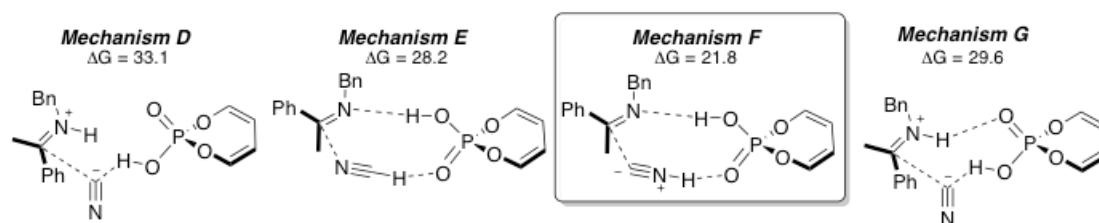

Figure 9. Calculated lowest energy transition states for the model catalyst. Energies[19] given in kcal mol^{-1}. The imine stereoisomer depicted was calculated to be lower in energy for this mechanism.

Model for Stereoselectivity

The models depicted in **Figure 7** are used to rationalise the stereoselectivities. In line with the model studies *N*-benzyl ketimines proceeded through a *Type I Z* transition state. Relative populations of transition states were predicted at 298 K from electronic energy differences and based on the Boltzmann distribution analysis. The calculation suggests that the *R* product should be formed in 58% enantiomeric excess in accordance with experiment although the absolute configuration was not determined. For benzaldehyde-derived benzyl imines the reaction proceeds via *Type I E* pathway,

agreeing with Rueping's original conformational analysis of the proposed interaction of the phosphate anion and the iminium ion. Although *Type I Z* transition states are more compact, the energy required to rotate the phenyl group is greater than the energy of the steric interactions with the 3,3' substituents.

PHOSPHORIC ACID CATALYZED FRIEDEL-CRAFTS REACTION

The bifunctional mechanism can also be applied to the Friedel-Crafts reaction as proposed by Zhou, supported by experimental studies.[11] The group noted that protecting the indole lead to no reaction, supporting the importance of a productive binding site to the catalyst *via* a hydrogen bond to this position. Indeed, such a strategy has become a standard experimental test of the bifunctional mechanism. In each of the reactions studied so far, the nucleophile has been symmetrical, unlike indole.[16,19] Focussing our efforts on two literature examples reported by Zhou[11] and You[38] (**Figure 10**), we expanded our model (**Figure 7**) to account for the stereoselective outcome of such reactions.[20] There are sixteen reasonable diastereomeric transition states for these reactions, resulting from *Type I* or *Type II* pathways, four different arrangements of the imine and two orientations of the indole. Our model studies allowed us to reduce this number to eight, as the energy differences between the *E* and *Z* configurations are so large that not even the catalyst steric interactions could change this preference.
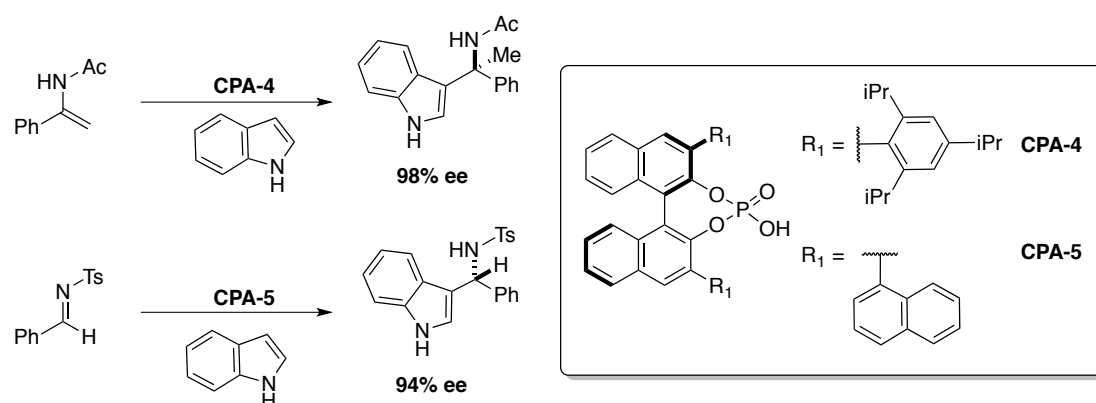
Figure 10. Friedel-Crafts reactions of indole and imines reported by the groups of Zhou[11] and You[38].

Model for Stereoselectivity

In both reactions only four of the transition states are significant for the prediction of stereoselectivity. There were two possible arrangements of imines, *Type I* and *Type II* and two possible arrangements of the nucleophile, *exo* and *endo*. In the lowest energy transition state structures, the large indole is directed to one side of the catalyst that is not occupied by the bulky catalyst group, minimising steric interactions. The lowest TS corresponds to a *Type II* pathway; in this conformation the acyl group is directed towards the 3,3' but the steric interactions are reduced as the imine tilts. This allows the largest substituent, the phenyl group, to be placed furthest from the bulk of the 3,3' substituents. Larger *N*-substituents adopt a similar tilted disposition, but the interactions with the 3,3' substituent and this larger group are much more costly. As shown in **Figure 11** the *Type I* pathway with tosyl-imines is now highly favored. In agreement with experiments a reversal in stereochemistry is expected (**Figure 10**).
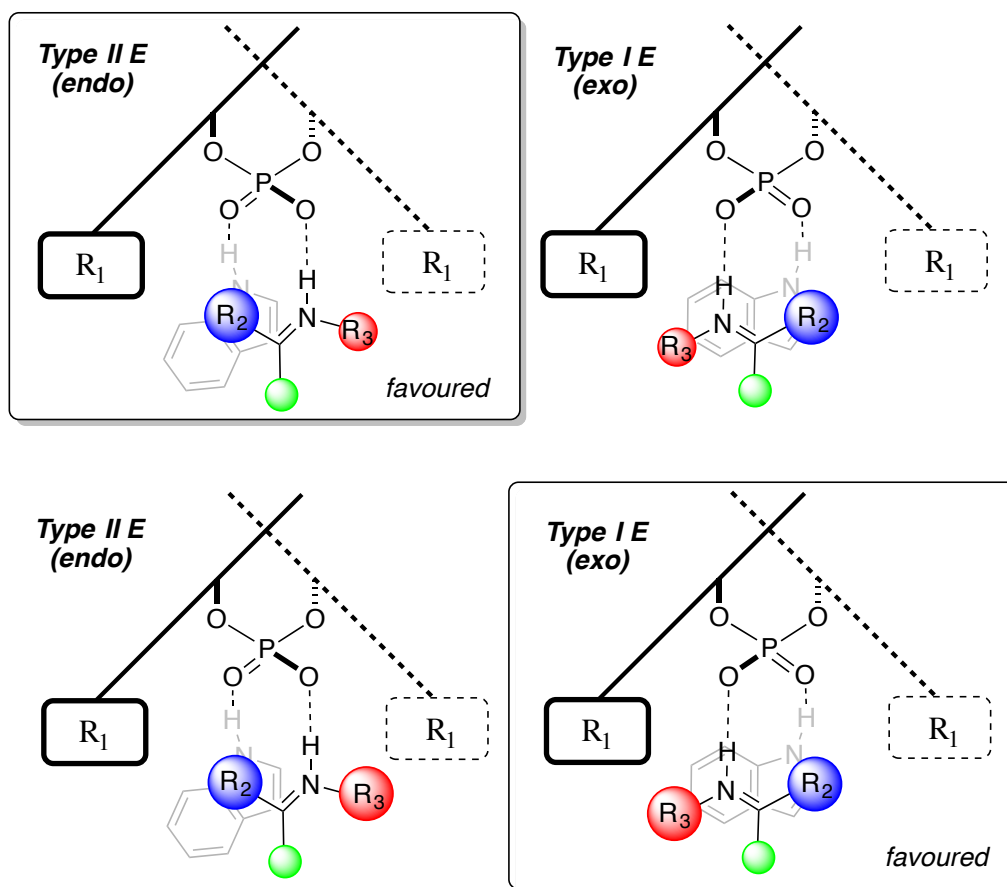
Figure 11. Models to predict the enantioselectivity in Friedel-Crafts reactions of indoles to acyl-ketimines (top) and tosyl-aldimines (bottom).

USING THE MODEL TO PREDICT STEREOSELECTIVITIES

The models for stereoselectivity depicted in **Figure 7** not only predict the stereoselectivity of the reactions described above, but can also be used to rationalise the stereochemical outcome of many nucleophilic additions to imines. Combining all possible considerations, a total of four possible transition state pathways are formulated and, as demonstrated above not all reactions proceed *via* the same one. Through detailed DFT calculations and literature results we have generalised and summarized which effects dictate the favored reaction pathway allowing the model to become a powerful predictive tool. In general most reactions proceed *via Type I E*

pathways. However, this preference can be modulated by the sterics of the reactants. In the next section we discuss our guiding principles to reaction pathway classification and give an overview of reactions for which it is useful.

_E_ or _Z_ transition state: Imine Configuration

_E_ imines are more stable than _Z_ imines and this energy difference is maintained in the transition state. Consequently, aldimines have a larger difference between the _E_ and _Z_ forms and so proceed _via E_ transition state pathways. Early mechanistic studies by Terada _et al_. suggested a mono-activation mechanism could be in operation in the Mannich reaction.[14] Guided by calculations on the pre-reaction complexes of the phosphoric acid catalyst and the imine (B3LYP/6-31G* geometry optimizations), Terada proposed two diastereomeric transition states. Both featured a single hydrogen bond to the _E_-imine. Structure **6** would be disfavored due to steric clashing between Boc and the large 3,3' substituents (**Figure 12**). Addition of acetylacetone to the less-hindered face would afford the major enantiomer. In accord with our previous DFT studies[16,19-21] and those of others[30,32,34,39-41] we conclude that the electrophile and nucleophile are activated simultaneously, creating a rigid network capable of inducing high enantioselectivity. The successful realisation of such a strategy constituted a highly general method of addition of protic nucleophiles to imines summarized in **Figures 13, 14**, **16** and **17**.
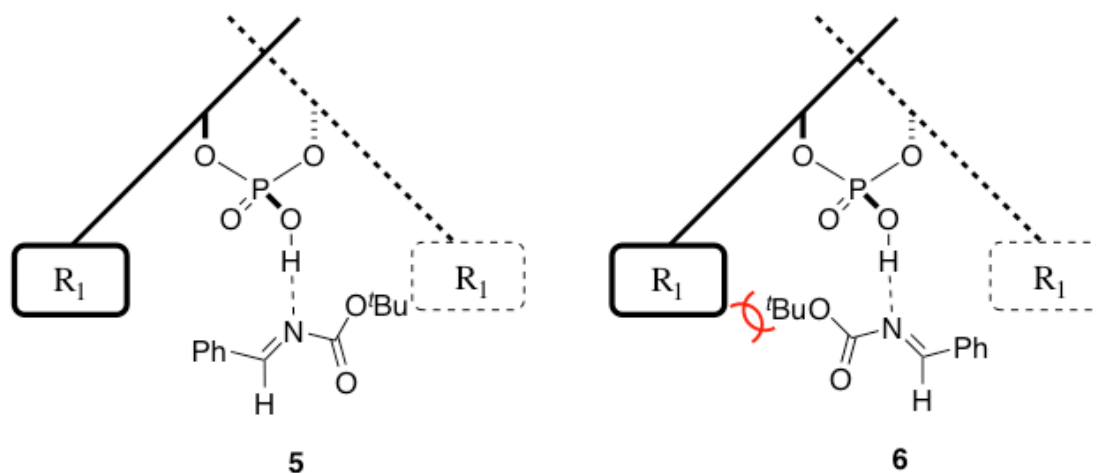
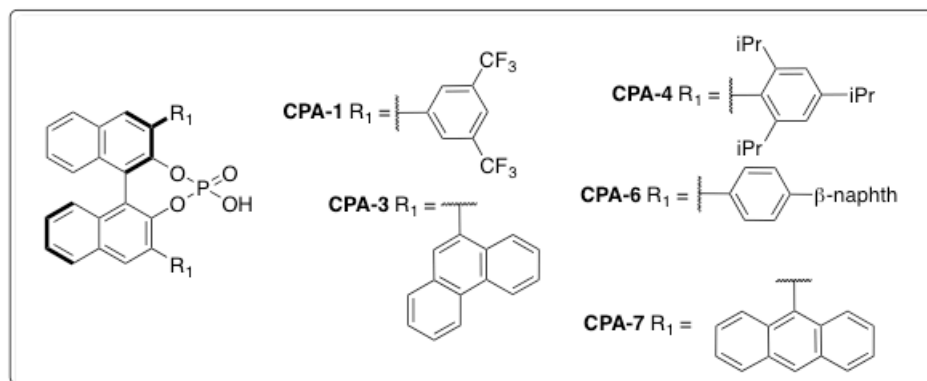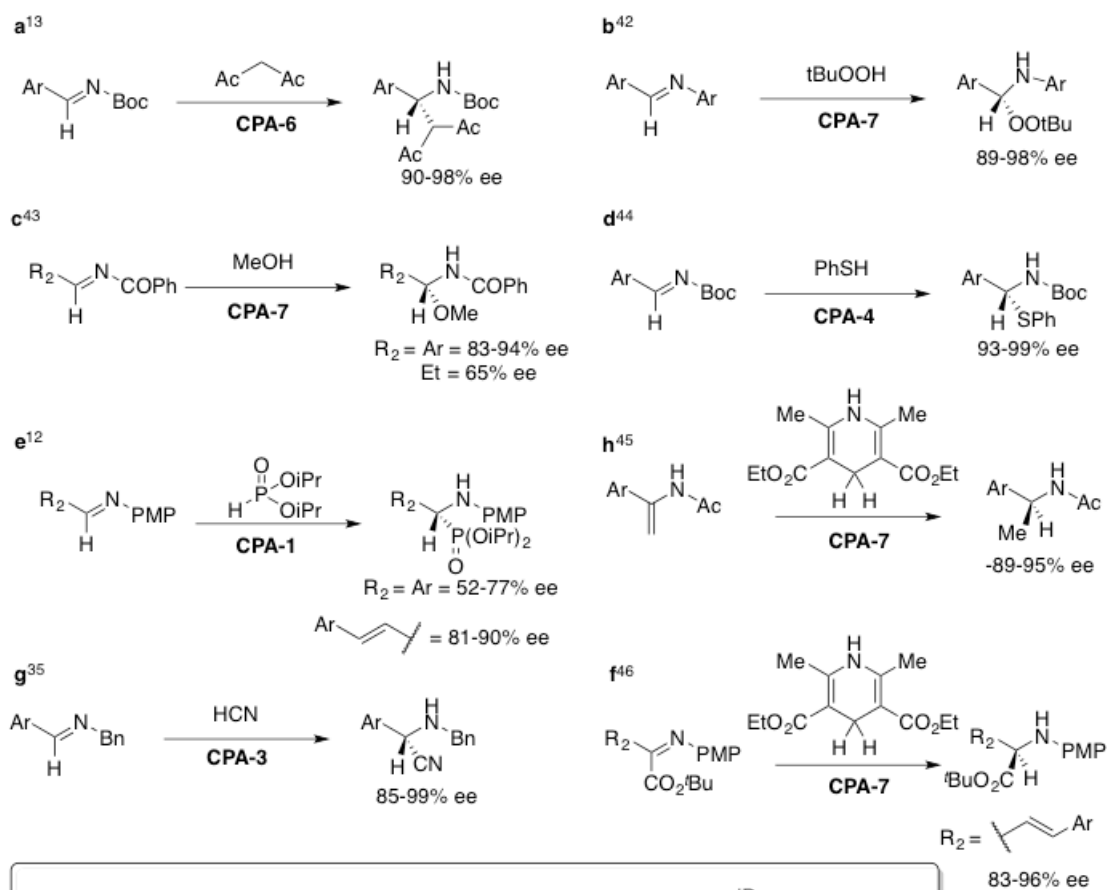**Figure 12**. Proposed models for stereoselectivity for Mannich reaction.

Figure 13. Summary of reactions that proceed *via E* pathways.

Ketimines have a smaller energy difference between *E* and *Z* forms and both pathways are possible. While acyclic substrates can freely equilibrate, cyclic substrates are locked in a *Z* configuration and can only proceed *via Z* pathways.
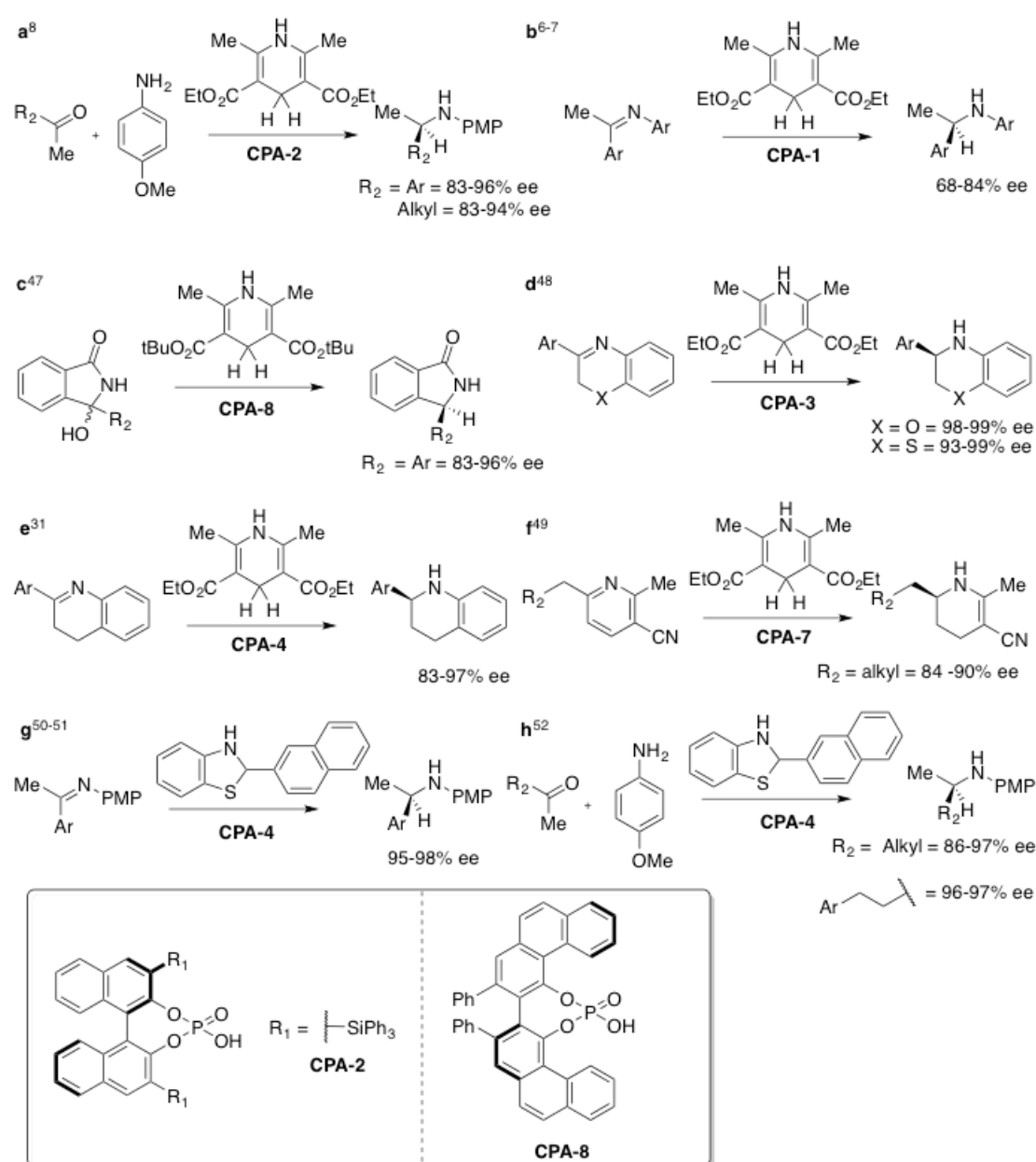

Figure 14. Examples of reactions that proceed *via Z* pathways.

Our previous study into the origin of stereoinduction based on substrate structure has suggested that structure of the starting material can be used to provide stereochemical information about the transition state.[21] Specifically, our study showed that if the ground state energy difference between the *E* and *Z* imine was large, the *E* transition state prevailed. In contrast, if there was a relatively small energy difference the reaction generally proceeded *via* the *Z* imine. This guideline allows a prediction of the preferred transition state to be made from analysis of the ground state preference of the imine, which is generally much easier to calculate or to estimate. This simple model is able to capture a number of results that are neither intuitive nor predictable. In 2009 Antilla *et al.* reported the transfer hydrogenation of enamides.[45] The stereochemical outcome is consistent with a *Type I E* pathway except for two examples, one of which was the reduction of (2-methoxyphenyl)-methyl-ketone derivative. The major compound has the opposite stereochemistry and lower enantiomeric excess (ee) than if the acetophenone derived enamide was reduced. It was not altogether clear why such a small structural modification could lead to such a dramatic change in result. On the basis of this, ONIOM calculations were performed, considering all possible pathways. It was found that the preferred pathway changed from *Type I E* to *Z*.[21] Such a change is captured with our model. The high energy difference between the *E/Z* imine and its protonated counterpart for **7** suggests that *E* selectivity will be good and the dramatically reduced *E* preference suggests that *E/Z* selectivity will be poor for **8** (**Figure 15**). Although ground state preference of the imine has a big impact on the *E/Z* preference of TS structures, this preference is also determined by the relative stability of the product conformation that followed in the reaction path. Based on QRC calculations, which connect transition states with their

corresponding ground states,[53] an approximation of a TS structure could be obtained by "averaging" the geometries of the minima from the reactant side and in the product side. Therefore, a fraction of all factors that stabilizes (or destabilizes) the reactants are present in the TS, because the TS still resembles the reactants. But with the same reasoning, a fraction of all factors that stabilizes (or destabilizes) the product are also noticed in the TS structure. An earlier TS structure will be less sensitive to these factors based on the Hammond postulate. It was determined that the product conformations obtained from *Z* TS structures were more stable than those from *E* TS structures. This information is not helpful in building a model for predicting the enantioselectivity but was essential in understanding that the most stable reactant is not always the one favored in the reaction process. A thorough study of eighteen substrates and three different reactions concluded that the aldimine transition state structures are always *E* and methyl ketimine transition state structures favour *Z*, unless the mean imine/iminium *E* structures are preferred to *Z* structures by more than 3 kcal mol^{-1}.
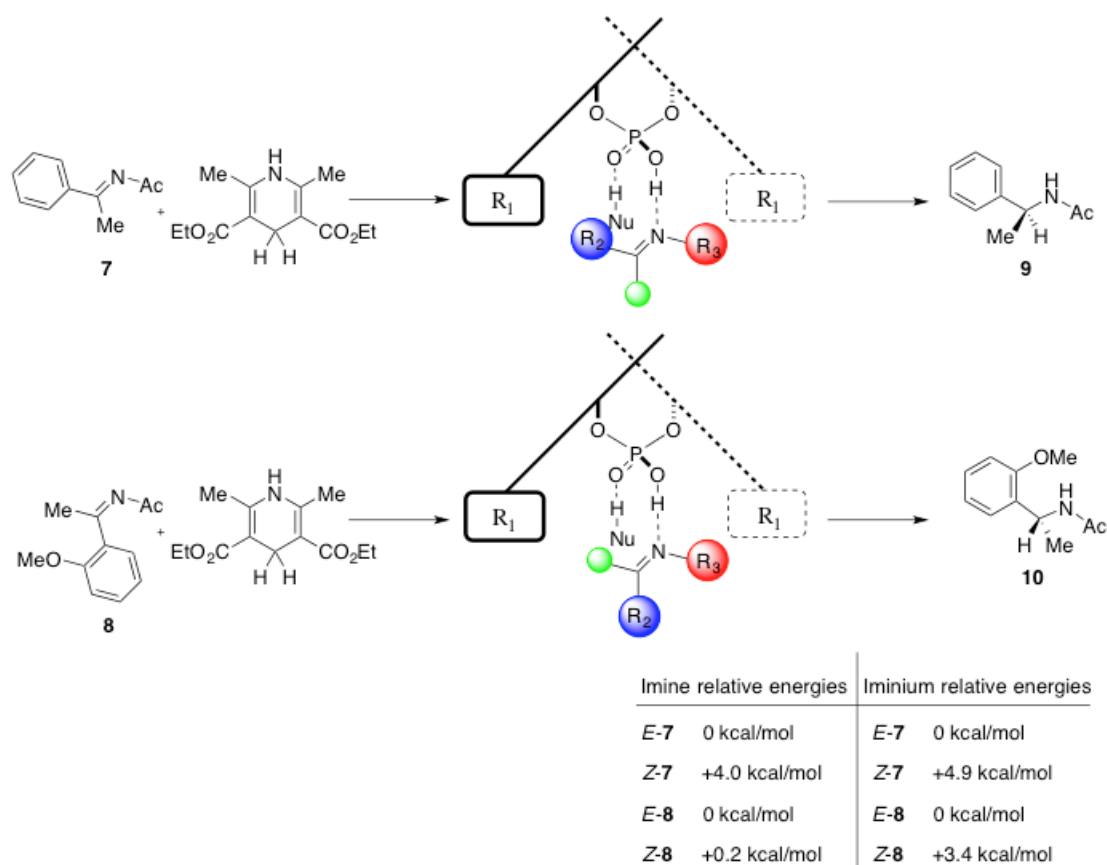
Figure 15. Prediction of reaction pathway based on the assumption that the transition state geometry is between that of the imine and iminium.

Type I or *Type II* transition state: nature of the nucleophile

For most nucleophiles, such as HCN and the Hantszch ester, the H-bond that holds the nucleophile to the catalyst is in line with nucleophilic site. However, in some cases the bond may be displaced to one side. Examples of such nucleophiles include the indoles: the nucleophilic carbon is not in line with the H-bond. This can promote a *Type II* process, but only if it is reinforced by a small *N*-imine and a large coplanar substituent.
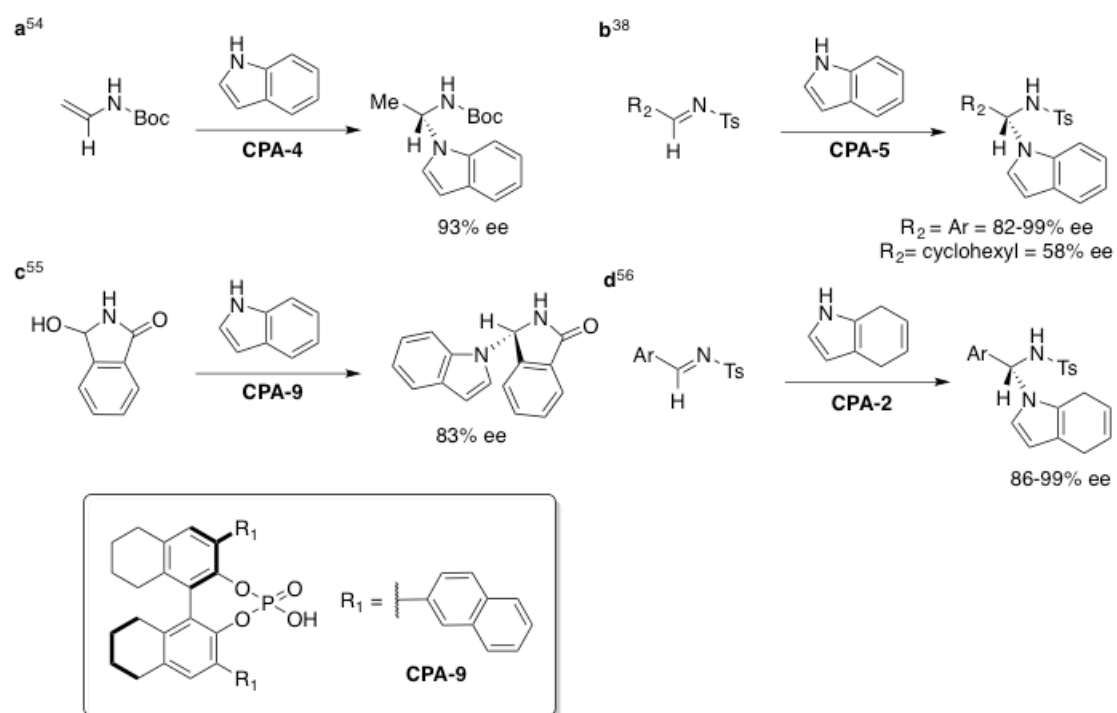
Figure 16. Examples of reactions that proceed *via Type I* pathways with displaced nucleophiles.
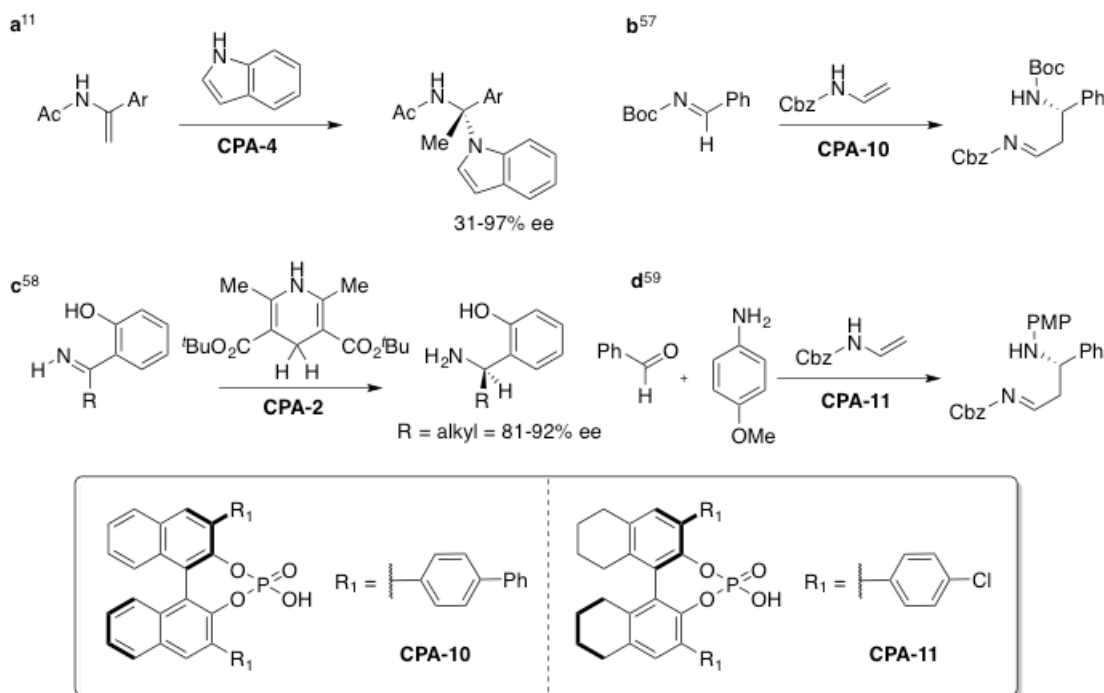
Figure 17. Examples of reactions that proceed *via Type II* pathways.

Enamide derived nucleophiles fall into this class and generally proceed through *Type II* pathways. One intriguing example was the reversal of stereochemistry with ene-carbamates and acyl imines (**Figure 18**). Calculations show that the same type of effects governs the stereochemistry. For reaction (a),[60] the *Type II* TS is preferred: the Cbz group on the nucleophile is large and pushes the sterically less demanding nucleophilic carbon toward the right-hand side of the catalyst. The phenyl group (R_2) of the imine electrophile needs more space on the right-hand side than the Boc group (R_3) that can rotate the tert-butyl group out of the way. R_3, therefore, is less sterically demanding than R_2. The corresponding *Type I* transition structure has a higher energy because the phenyl of the imine and the Cbz of the nucleophile have unfavorable steric interactions with the BINOL-phosphoric acid substituents. For reaction (b),[10] the *Type I* pathway is lower in energy; in this case the benzoyl *N*-substituent is sterically more demanding than the phenyl group.
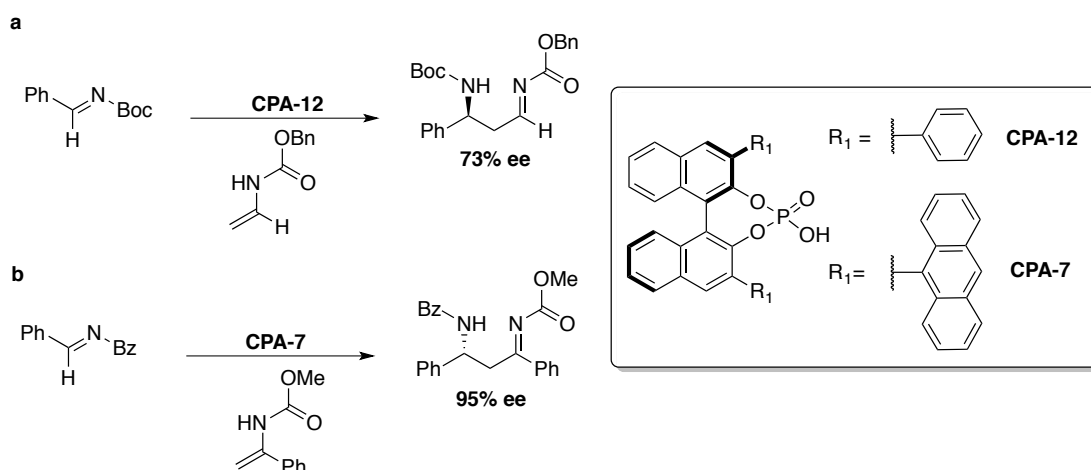
Figure 18. Addition of enecarbamates to imines.

Based on our theoretical studies and the literature results we have summarized the factors that contribute to the reaction pathway in **Figure 19**. The reactants follow either the right hand or left hand pathways, and the choice is controlled by the four factors listed: R_3 size, R_2 size, nucleophile type and imine configuration. The underlying feature of the pathways is the desire for the reactants to minimise steric interactions with the 3,3' substituents. It is, therefore, unsurprising that large *N*-imine substituents (R_3 in **Figure 19**) favor *Type I* processes and small substituents bias towards *Type II*. Similarly, a large group on the other end of the imine (R_2) would also avoid the 3,3' substituents and so a large R_2 favors *Type II*. The nature of the nucleophile is also very important: displaced nucleophiles, such as indole, favor *Type II* processes. A *Z* transition state makes it possible to placing two large groups away from the majority of the steric bulk. However, to proceed through such a pathway the configuration will need to be accessible. The likelihood of a *Z* transition state can be estimated from the energy difference between the *E* and *Z* imine ground states. An energy difference of less than 3 kcal mol^{-1} in favor of the *E* ground state suggests that a *Z* preference is possible.
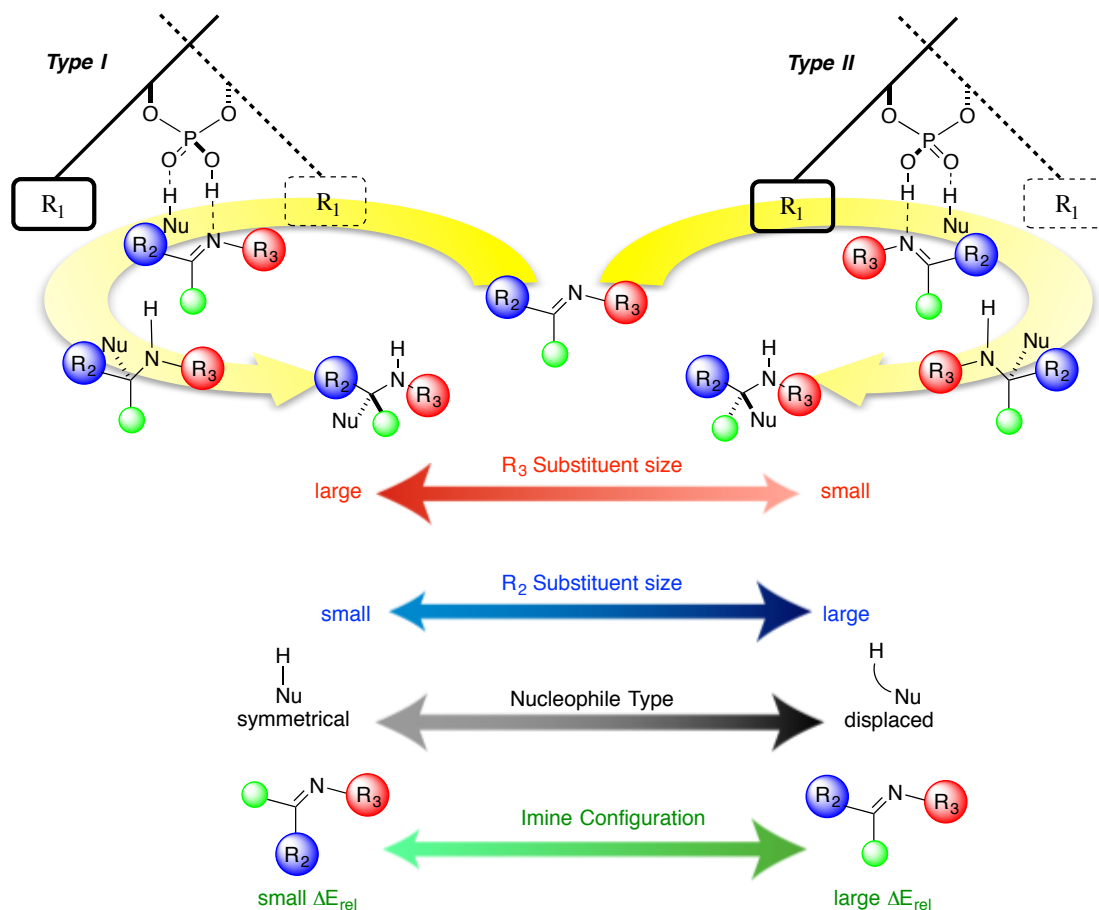
Figure 19. Reaction pathway spectrum. The effects of various features on the stereoselective outcome are shown.

CONCLUSION

Computational methods have become increasingly useful for modelling catalytic reactions. Such methods have evolved to provide new understanding of experimental

results, with detailed insights into mechanisms and origins of stereoinduction. However, for many-atom systems, it was impractical to study reactions by very accurate methods until it became possible to use ONIOM approaches. Rationalising the outcome and enantiomeric excesses of these complex reactions is now feasible. Summarising the calculations into a simple qualitative model, **Figure 19**, represents a powerful tool for predicting the stereochemical outcome of phosphoric acid catalyzed nucleophilic additions to imines and is a quick and easy method for the prediction of reaction pathway and stereoselectivity.

BIOGRAPHICAL INFORMATION

Jolene Reid obtained her MSci degree from Queens University Belfast in 2013. She is currently a PhD student with Jonathan Goodman at Cambridge.

Luis Simón received his PhD in organic chemistry from the University of Salamanca in 2005. He is currently lecturer in the Chemical Engineering Department of the University of Salamanca. His research interests include theoretical investigation of organocatalytic reactions and host-guest chemistry.

Jonathan Goodman did experiments on aldol reactions during his PhD with Ian Paterson at the University of Cambridge, and then was a post-doc with Clark Still at Columbia University, before returning to Cambridge, where he is now Professor of Chemistry.

REFERENCES

[1] Klussmann, M.; Ratjen, L.; Hoffmann, S.; Wakchaure, V.; Goddard, R.; List, B. Synthesis of TRIP and Analysis of Phosphate Salt Impurities. *Synlett,* **2010**, *14*, 2189-2192.

[2] Akiyama, T. Stronger Brønsted Acids. *Chem. Rev.* **2007**, *107*, 5744–5758.

[3] Terada, M. Chiral Phosphoric Acids as Versatile Catalysts for Enantioselective Transformations. *Synthesis,* **2010**, 1929–1982.

[4] Rueping, M.; Kuenkel, A.; Atodiresei, I. Chiral Brønsted Acids in enantioselective carbonyl activations – activation modes and applications. *Chem. Soc. Rev.* **2011**, *40*, 4539–4549.

[5] Parmar, D., Sugiono, E., Raja, S. and Rueping, M. Complete Field Guide to Asymmetric BINOL-Phosphate Derived Brønsted Acid and Metal Catalysis: History and Classification by Mode of Activation; Brønsted Acidity, Hydrogen Bonding, Ion Pairing, and Metal Phosphates. *Chem. Rev.* **2014**, *114,* 9047-9153.

[6] Rueping, M.; Sugiono, E.; Azap, C.; Theissmann, T.; Bolte, M. Enantioselective Brønsted Acid Catalyzed Transfer Hydrogenation: Organocatalytic Reduction of Imines. *Org. Lett*. **2005**, *7*, 3781-3783.

[7] Hoffmann, S.; Seayad, A. M.; List, B. A Powerful Brønsted Acid Catalyst for the Organocatalytic Asymmetric Transfer Hydrogenation of Imines. *Angew. Chem. Int. Ed.* **2005**, *44,* 7424-7427.

[8] Storer, R. I.; Carrera, D. E.; Ni, Y.; MacMillan, D. W. C. Enantioselective Organocatalytic Reductive Amination. *J. Am. Chem. Soc*. **2006**, *128*, 84-86.

[9] Guo, Q.-X.; Liu, H.; Guo, C.; Luo, S.-W.; Gu, Y.; Gong, L.-Z. Chiral Brønsted Acid-Catalyzed Direct Asymmetric Mannich Reaction. *J. Am. Chem. Soc.* **2007**, *129*, 3790–3791.

[10] Terada, M.; Machioka, K.; Sorimachi, K. High Substrate/Catalyst Organocatalysis by a Chiral Brønsted Acid for an Enantioselective Aza-Ene-Type Reaction. *Angew. Chem. Int. Ed.* **2006**, *45*, 2254–2257.

[11] Jia, Y.-X.; Zhong, J.; Zhu, S.-F.; Zhang, C.-M.; Zhou, Q.-L. Chiral Brønsted Acid Catalyzed Enantioselective Friedel–Crafts Reaction of Indoles and α-Aryl Enamides: Construction of Quaternary Carbon Atoms. *Angew. Chem. Int. Ed*. **2007**, *46*, 5565–5567.

[12] Akiyama, T.; Morita, H.; Itoh, J.; Fuchibe, K.Chiral Brønsted Acid Catalyzed Enantioselective Hydrophosphonylation of Imines: Asymmetric Synthesis of α-Amino Phosphonates. *Org. Lett.* **2005**, *7*, 2583–2585.

[13] Uraguchi, D.; Terada, M. Chiral Brønsted Acid-Catalyzed Direct Mannich Reactions *via* Electrophilic Activation. *J. Am. Chem. Soc.* **2004**, *126*, 5356-5357.

[14] Gridnev, I. D.; Kouchi, M.; Sorimachi, K.; Terada, M. On the mechanism of stereoselection in direct Mannich reaction catalyzed by BINOL-derived phosphoric acids. *Tetrahedron Lett*. **2007**, *48*, 497–500.

[15] Yamanaka, M.; Itoh, J.; Fuchibe, K.; Akiyama, T. Chiral Brønsted Acid Catalyzed Enantioselective Mannich-Type Reaction *J. Am. Chem. Soc.* **2007**, *129*, 6756-6764.

[16] Simón, L.; Goodman, J. M. Theoretical Study of the Mechanism of Hantzsch Ester Hydrogenation of Imines Catalyzed by Chiral BINOL-Phosphoric Acids. *J. Am. Chem. Soc.* **2008**, *130,* 8741-8747.

[17] Johnson, J. E.; Morales, N. M.; Gorczyca, A. M.; Dolliver, D. D.; McAllister, M. A. Mechanisms of acid-catalyzed Z/E isomerization of imines. *J. Org. Chem.* **2001**, *66*, 7979-7985.

[18] Chung, L. W.; Sameera, W. M. C.; Ramozzi, R.; Page, A. J.; Hatanaka, M.; Petrova, G. P.; Harris, T. V.; Li, X.; Ke, Z., Liu, F.; Li, H.-F.; Ding, L.; Morokuma, K. The ONIOM Method and Its Applications. *Chem. Rev.* **2015**, *115*, 5678−5796.

[19] Simón, L.; Goodman, J. M. Mechanism of BINOL-Phosphoric Acid-Catalyzed Strecker Reaction of Benzyl Imines. *J. Am. Chem. Soc.* **2009**, *131*, 4070-4077.

[20] Simón, L.; Goodman, J. M. DFT Study on the Factors Determining the Enantioselectivity of Friedel−Crafts Reactions of Indole with *N*-Acyl and *N*-Tosylimines Catalyzed by BINOL−Phosphoric Acid Derivatives. *J. Org. Chem.* **2010**, *75,* 589-597.

[21] Simón, L.; Goodman, J. M. A Model for the Enantioselectivity of Imine Reactions Catalyzed by BINOL-Phosphoric Acid Catalysts. *J. Org. Chem.* **2011**, *76,* 1775-1788.

[22] Grayson, M. N.; Pellegrinet, S. C.; Goodman, J. M. Mechanistic Insights into the BINOL-Derived Phosphoric Acid-Catalyzed Asymmetric Allylboration of Aldehydes. *J. Am. Chem. Soc.* **2012**, *134,* 2716-2722.

[23] Grayson, M. N.; Goodman, J. M. Understanding the Mechanism of the Asymmetric Propargylation of Aldehydes Promoted by BINOL-Derived Catalysts. *J. Am. Chem. Soc.* **2013**, *135,* 6142-6148.

[24] Overvoorde, L. M.; Grayson, M. N.; Luo, Y.; Goodman, J. M. Mechanistic Insights into a BINOL-Derived Phosphoric Acid-Catalyzed Asymmetric Pictet−Spengler Reaction. *J. Org. Chem.* **2015**, *80*, 2634−2640.

[25] Becke, A. D. Density-functional exchange-energy approximation with correct asymptotic behavior. *Phys. Rev.* A **1998**, *38*, 3098-3100.

[26] Lee, C.; Yang, W.; Parr, R. G. Development of the Colle-Salvetti correlation-energy formula into a functional of the electron density. *Phys. Rev. B* **1988**, *37*, 785-789.

[27] Johnson, E. R.; Mackie, I. D.; DiLabio, G. A. Dispersion interactions in density functional theory. *J. Phys. Org. Chem.* **2009**, *22*, 1127–1135.

[28] Zhao, Y.; Truhlar, D. G. The M06 suite of density functionals for main group thermochemistry, thermochemical kinetics, noncovalent interactions, excited states, and transition elements: two new functionals and systematic testing of four M06-class funtionals and 12 other functionals. *Theor. Chem. Acc.* **2008**, *120*, 215–241.

[29] Zhao, Y.; Truhlar, D. G. Density Functionals with Broad Applicability in Chemistry. *Acc. Chem. Res.* **2008**, *41*, 157–167.

[30] Marcelli, T.; Hammar, P.; Himo, F. Phosphoric Acid Catalyzed Enantioselective Transfer Hydrogenation of Imines: A Density Functional Theory Study of Reaction Mechanism and the Origins of Enantioselectivity. *Chem. Eur. J.* **2008**, *14,* 8562-8571.

[31] Rueping, M.; Antonchick, A. P.; Theissmann, T. A Highly Enantioselective Brønsted Acid Catalyzed Cascade Reaction: Organocatalytic Transfer Hydrogenation of Quinolines and their Application in the Synthesis of Alkaloids. *Angew. Chem. Int. Ed.* **2006**, *45*, 3683-3686.

[32] Shibata, Y.; Yamanaka, M. DFT Study of the Mechanism and Origin of Enantioselectivity in Chiral BINOL-Phosphoric Acid Catalyzed Transfer Hydrogenation of Ketimine and α-Imino Ester using Benzothiazoline. *J. Org. Chem.* **2013**, *78*, 3731-3736.

[33] Hoffmann, S.; Nicoletti, M.; List, B. Catalytic Asymmetric Reductive Amination of Aldehydes via Dynamic Kinetic Resolution. *J. Am. Chem. Soc.* **2006**, *128*, 13074-13075.

[34] Marcelli, T.; Hammar, P.; Himo, F. Origin of Enantioselectivity in the Organocatalytic Reductive Amination of α-Branched Aldehydes. *Adv. Synth. Catal*. **2009**, *351*, 525-529.

[35] Rueping, M.; Sugiono, E.; Azap, C. A Highly Enantioselective Brønsted Acid Catalyst for the Strecker Reaction. *Angew. Chem. Int. Ed*. **2006**, *45*, 2617-2619.

[36] Rueping, M.; Sugiono, E.; Moreth, S. A. Metal-Free, Enantioselective Strecker Reactions Catalyzed by Chiral BINOL and TADDOL Catalysts. *Adv. Synth. Catal.* **2007**, *349*, 759-764.

[37] Li, J.; Jiang, W.-Y.; Han, K.-L.; He, G.-Z.; Li, C. Density Functional Study on the Mechanism of Bicyclic Guanidine-Catalyzed Strecker Reaction. *J. Org. Chem.* **2003**, *68*, 8786–8789.

[38]Kang, Q.; Zhao, Z.-A.; You, S.-L. Highly Enantioselective Friedel-Crafts Reaction of Indoles with Imines by a Chiral Phosphoric Acid. *J. Am. Chem. Soc.* **2007**, *129*, 1484-1485.

[39] Akiyama, T.; Morita, H.; Bachu, P.; Mori, K.; Yamanaka, M.; Hirata, T. Chiral Brønsted acid-catalyzed hydrophosphonylation of imines—DFT study on the effect of substituents of phosphoric acid. *Tetrahedron* **2009**, *65*, 4950-4956.

[40] Yamanaka, M.; Hirata, T. DFT Study on Bifunctional Chiral Brønsted Acid-Catalyzed Asymmetric Hydrophosphonylation of Imines**.** *J. Org. Chem.* **2009**, *74*, 3266-3271.

[41] Shi, F.-Q.; Song, B.-A. Origins of enantioselectivity in the chiral Brønsted acid catalyzed hydrophosphonylation of imines. *Org. Biomol. Chem.* **2009**, *7*, 1292-1298.

[42] Zheng, W.; Wojtas, L.; Antilla, J. C. Chiral Phosphoric Acid Catalyzed Peroxidation of Imines. *Angew. Chem. Int. Ed.* **2010**, *49*, 6589-6591.

[43] Li, G.; Fronczek, F. R.; Antilla, J. C. Catalytic Asymmetric Addition of Alcohols to Imines: Enantioselective Preparation of Chiral N,O-Aminals. *J. Am. Chem. Soc.* **2008**, *130*, 12216–12217.

[44] Ingle, G. K.; Mormino, M. G.; Wojtas, L.; Antilla, J. C. Chiral Phosphoric Acid-Catalyzed Addition of Thiols to *N*-Acyl Imines: Access to Chiral *N,S*-Acetals. *Org. Lett*. **2011**, *13*, 4822-4825.

[45] Li, G.; Antilla, J. C. Highly Enantioselective Hydrogenation of Enamides Catalyzed by Chiral Phosphoric Acids. *Org. Lett.* **2009**, *11*, 1075-1078.

[46] Kang, Q.; Zhao, Z.-A.; You, S.-L. Asymmetric Transfer Hydrogenation of β,γ-Alkynyl α-Imino Esters by a Brønsted Acid. *Org. Lett*. **2008**, *10*, 2031-2034.

[47] Chen, M.-W.; Chen, Q.-A.; Duan, Y.; Ye, Z.-S.; Zhou, Y.-G. Asymmetric hydrogenolysis of racemic tertiary alcohols, 3-substituted 3-hydroxyisoindolin-1-ones. *Chem. Commun*. **2012**, *48*, 1698-1700.

[48] Rueping, M.; Antonchik, A. P.; Theissmann, T. Remarkably Low Catalyst Loading in Brønsted Acid Catalyzed Transfer Hydrogenations: Enantioselective Reduction of Benzoxazines, Benzothiazines, and Benzoxazinones. *Angew. Chem. Int. Ed.* **2006**, *45*, 6751-6755.

[49] Rueping, M.; Antonchick, A. P. Organocatalytic Enantioselective Reduction of Pyridines. *Angew. Chem. Int. Ed.* **2007**, *46*, 4562-4565.

[50] Zhu, C.; Akiyama, T. Benzothiazoline: Highly Efficient Reducing Agent for the Enantioselective Organocatalytic Transfer Hydrogenation of Ketimines. *Org. Lett.* **2009**, *11*, 4180-4183.

[51] Saito, K.; Horiguchi, K.; Shibata, Y.; Yamanaka, M.; Akiyama, T. Chiral Phosphoric-Acid-Catalyzed Transfer Hydrogenation of Ethyl Ketimine Derivatives by Using Benzothiazoline. *Chem. Eur. J.* **2014**, *20*, 7616 – 7620.

[52] Saito, K.; Akiyama, T. Enantioselective organocatalytic reductive amination of aliphatic ketones by benzothiazoline as hydrogen donor. *Chem. Commun.* **2012**, *48*, 4573-4575.

[53] Silva, M. A.; Goodman, J. M. QRC: A rapid method for connecting transition structures to reactants in the computational analysis of organic reactivity. *Tetrahedron Lett.* **2003**, *44*, 8233-8236.

[54] Terada, M.; Sorimachi, K. Enantioselective Friedel−Crafts Reaction of Electron-Rich Alkenes Catalyzed by Chiral Brønsted Acid. *J. Am. Chem. Soc.* **2007**, *129*, 292-293.

[55] Yu, X.; Wang, Y.; Wu, G.; Song, H.; Zhou, Z.; Tang, C. Organocatalyzed Enantioselective Synthesis of Quaternary Carbon-Containing Isoindolin-1-ones. *Eur. J. Org. Chem.* **2011**, *2011*, 3060-3066.

[56] Kang, Q.; Zheng, X.-J.; You, S.-L. Highly Enantioselective Friedel–Crafts Reaction of 4,7-Dihydroindoles with Imines by Chiral Phosphoric Acids: Facile Access to 2-Indolyl Methanamine Derivatives. *Chem. Eur. J.* **2008**, *14*, 3539 − 3542.

[57] Terada, M.; Machioka, K.; Sorimachi, K. Chiral Brønsted Acid-Catalyzed Tandem Aza-Ene Type Reaction/Cyclization Cascade for a One-Pot Entry to Enantioenriched Piperidines. *J. Am. Chem. Soc.* **2007**, *129*, 10336-10337.

[58] Nguyen, T. B.; Bousserouel, H.; Wang, Q.; Guéritte, F. Chiral Phosphoric Acid-Catalyzed Enantioselective Transfer Hydrogenation of *ortho*-Hydroxyaryl Alkyl N−H Ketimines. *Org. Lett.* **2010**, *12*, 4705-4707.

[59] Liu, H.; Dagousset, G.; Masson, G.; Retailleau, P.; Zhu, J. Chiral Brønsted Acid-Catalyzed Enantioselective Three-Component Povarov Reaction. *J. Am. Chem. Soc.* **2009**, *131*, 4598-4599.

[60] Terada, M.; Machioka, K.; Sorimachi, K. Activation of Hemiaminal Ethers by Chiral Brønsted Acids for Facile Access to Enantioselective Two-Carbon Homologation Using Enecarbamates. *Angew. Chem. Int. Ed*. **2009**, *48*, 2553-556.